



PARAMETRIC STUDY OF SUCTION OR BLOWING EFFECTS ON TURBULENT FLOW OVER A FLAT PLATE

Prof.Dr. Najdat Nashat Abdulla & Miss.Sajida Lafta Ghashim Jassim
University of Baghdad
College of Engineering
Mechanical Engineering Department

ABSTRACT

The two-dimensional, incompressible, and turbulent boundary layer flow over a flat plate with suction or blowing from a spanwise slot is examined numerically. The mathematical modeling involves the derivation of the governing partial differential equations of the problems. These are the continuity, the momentum, the energy and the (K- ϵ) turbulence model. Besides, the perfect gas law is also used. A numerical solution of the governing equations is approximated by using a finite volume method, with staggered grid and modified SIMPLE algorithm. A computer program in FORTRAN 90 is built to perform the numerical solution. The developed computational algorithm is tested for the flow over a flat plate (4m) long with uniform suction or blowing velocity ratios of ($V/U_\infty = \pm 0.0185, \pm 0.0463$ and ± 0.0925 m/s) are imposed on the slot for Reynolds number of (1.36×10^7), based on the plate length. The position of the slot change in the range of ($X/L=1/4, 1/2$ and $3/4$) from leading edge and also, change width of slot in the value equal (0.12, 0.2 and 0.28m). The plate temperature is (70 °C), with the free stream velocity and temperature are (8.6m/s) and (25 °C) respectively. In addition, the effects of pitch angles on the flow field are investigated in the range of ($30^\circ \leq \alpha \leq 150^\circ$). The numerical results show that, for a uniform blowing, location of slot equal ($X/L=1/4$) from leading edge, a significant reduction of skin friction coefficient, wall shear stress and boundary layer thickness [displacement and momentum] to occur. While, an increase in boundary layer shape factor. Reynolds stress (uv) is more decreased than [(uu) and (vv)], mean velocity profiles in wall coordinates and dimensionless distance (U^+, y^+) decreases. When slot location is moved downstream to locations ($X/L=1/2$ or $3/4$) a similar behavior can be said and most effective slot is obtained as (slot at $X/L= 3m$) from leading edge. While width of slot equal (0.28m) is better than values equal (0.12m and 0.2m). An opposite observations for the case of suction. The numerical results are compared with available numerical results and experimental data and a satisfactory results are obtained.

الخلاصة

تم بحث جريان الطبقة المتاخمة المضطربة الثنائي البعد والأنضغاطي والمستقر على صفيحة مستوية مع وجود شق صغير دراسة عددية. يتضمن النموذج الرياضي اشتقاق المعادلات التفاضلية الجزئية للمسألة، والتي هي معادلات الاستمرارية، الزخم، الطاقة ومعادلة نموذج (K - ε) للاضطراب. بالإضافة إلى ذلك، تم استخدام معادلة الغاز المثالي. تم حل المعادلات عددياً باستخدام طريقة الحجوم المحددة (Finite Volume Method) مع الشبكة المزحفة (Staggered Grid) باستخدام خوارزمية (Simple Algorithm). تم بناء برنامج حاسوبي بلغة (FORTRAN 90) لإنجاز الحل العددي. النموذج العددي يتضمن الجريان على صفيحة مستوية طولها (4m) مع فرض نسب سرعة دفع أو سحب على الشق مقدارها (±0.0185, ±0.0463, ±) (V/U_∞=0.0925) لعدد رينولد (1.36×10⁷) وذلك بالاعتماد على طول الصفيحة. دراسة تأثير تغيير موقع الشق بمعدل (X/L=1/4, 1/2, 3/4) مع استعمال قيم مختلفة لعرض الشق (0.12, 0.2, 0.28m). درجة حرارة الصفيحة كانت (70°C) بينما كانت سرعة ودرجة حرارة الجريان الحر (8.6 m/s), (25°C) على التوالي. بالإضافة إلى ذلك، تم التحقق من تأثير زاوية الخطوة على حقل الجريان بحدود (30° ≤ α ≤ 150°). من خلال النتائج العددية نلاحظ أنه في حالة الدفع، عند اختيار موقع الشق بعيداً (X/L=1/4) عن مقدمة الصفيحة، نلاحظ نقصان معامل الاحتكاك، الاجهاد القصي مع نقصان سمك الطبقة المتاخمة (الزخم، السمك)، بينما معامل شكل الطبقة المتاخمة يزداد، اجهادات Reynolds (uv) أكثر نقصان من (uu) و (vv)، الأبعاد اللابعدية (U⁺, y⁺) تقل، وعندما يتم تسليط سرعة الدفع من خلال شق آخر يبعد عن مقدمة الصفيحة مثلاً (X/L=1/4, 1/2) نلاحظ أنه نفس الشيء يحدث وأفضل موقع فعال يبعد (X/L=3/4). أما مقدار الشق الذي يساوي (0.28m) أفضل من بقية القيم الأخرى التي تساوي (0.12, 0.2m) عكس الشيء يمكن ملاحظته في حالة السحب. وتم مقارنة النتائج العددية مع النتائج العددية والعملية المتوفرة وكانت نتائج المقارنة مقاربة مع اختلاف بسيط مع النتائج العددية.

KEY WORD: Local forcing, Turbulent boundary layer, effect of suction and blowing, Drag reduction, Boundary layer control.

INTRODUCTION

A turbulent boundary layer is one of the wall turbulence flows that affected by the presence of solid wall. According to experimental data, a turbulent boundary layer made up of inner and outer regions. The effects of wall suction or blowing have been studied experimentally and numerically, the physics of a blowing or suction boundary layer is in fact mostly a no slip boundary layer that is perturbed slightly by the addition / extraction of a small amount of fluid. Literature survey reveals that several methods have been done to investigate the effect of suction and blowing numerically and numerically by the authors:

Park and Choi [1999] studied the effects of uniform blowing and suction over a flat plate on a turbulent boundary layer flow using the direct numerical simulation technique. The integration method used to solve Navier-Stokes equations. The magnitudes of blowing or suction are less than 10% of the free- stream velocity. The skin friction and near- wall turbulence intensities are significantly changed by blowing and suction. In the case of uniform blowing, the skin friction on the slot rapidly decreases. The streamwise vortices above the wall are lifted up by blowing, and thus the interaction of the vortices with the wall becomes weaker. Accordingly, the lifted vortices become stronger in the downstream due to less viscous diffusion (above the slot) and more tilting and stretching (downstream of the slot), resulting in the increase of the turbulence intensities as well as the skin friction downstream of the slot. The opposite is observed in the case of uniform suction. For both cases of blowing and suction, the streamwise turbulence intensity recovers quickly from blowing or suction, while other components of the turbulence intensities and Reynolds shear stress recover in a longer downstream distance.

Kim and Sung [2003] investigated the effects of time-periodical blowing through a spanwise slot on a turbulent boundary layer. The blowing velocity was varied in a cyclic manner from 0 to $2A^+$ ($A^+ = 0.25, 0.50, \text{ and } 1.00$) at a fixed blowing frequency of $f^+ = 0.017$. The effect of steady blowing (SB) was also examined, and the SB results were compared with those for periodic blowing (PB). PB reduced the skin friction near the slot, although to a slightly lesser extent than SB. PB was found to generate a spanwise vertical structure in the downstream of the slot. This vortex generates a reverse flow near the wall, there by reducing the wall shear stress. The wall- normal and spanwise turbulence intensities under PB are increased as compared to those under SB, whereas the streamwise turbulent intensity under PB is weaker than that under SB. PB enhances more energy redistribution than SB. The periodic response of the streamwise turbulence intensity to PB is propagated to a lesser extent than that of the other components of the turbulence intensities and the Reynolds shear stress.

Munem [2004] developed a general method for numerical solution of the steady state, two dimensional and incompressible turbulent flow over a flat plate with uniform suction or blowing. Turbulence effect was handled through considering K- ϵ model. The solution algorithm SIMPLE in cartesian coordinates system with staggered grid technique was used to solve the Navier- Stokes equations with continuity equation. The results show that, for uniform blowing, the skin friction rapidly decreases near the slot and increases in the downstream of the slot, the most effective pitch angle is obtained as ($\alpha = 60^\circ$) which gives the maximum reduction of skin friction coefficient. Near the blowing slot, the velocity fluctuations and Reynolds shear stress decrease, because their profiles are shifted away from the wall. An opposite observations are obtained for the case of suction velocities. Results were compared with available numerical and experimental data show a good agreement.

Krogstad and Kourakine [2000] investigated the effects of localized injection through a porous strip on a turbulent boundary layer at zero pressure gradient conditions experimentally. The magnitude of the injection velocity were kept very small (less than 1% of the free-stream velocity) to prevent separation near the injection strip and to keep the perturbations small. It was found that, the injection increases all the Reynolds stresses and, this perturbation dies out very slowly as the affected layer is sandwiched between the outer edge of the incoming boundary layer and a new layer that develops at the wall. A study of the anisotropy tensor indicated no effects of the blowing rate on the flow anisotropy downstream of the injection region.

Park, Park and Sung [2003] performed an experimental study to investigate the effect of periodic blowing and suction on a turbulent boundary layer. Partical Image Velocimetry (PIV) was used to probe the characteristics of the flow. Local forcing was introduced to the boundary layer via a sinusoidally – oscillating jet issuing from a thin spanwise slot. Three forcing frequencies ($f^+ = 0.044, 0.066, \text{ and } 0.088$) with a fixed forcing amplitude ($A^+ = 0.6$) were employed at $Re_\theta = 690$. The effect of three different forcing angles ($\alpha = 60^\circ, 90^\circ \text{ and } 120^\circ$) was investigated under a fixed forcing frequency ($f^+ = 0.088$). The PIV results showed that, the wall- region velocity decreases on imposition of the local forcing. Inspection of the phase- averaged velocity profiles revealed that, spanwise large- scale vortices are generated downstream of the slot and persist father downstream. The highest reduction in skin friction was achieved at the highest forcing frequency ($f^+ = 0.088$) and a forcing angle of ($\alpha = 120^\circ$). The spatial fraction of the vortices was examined to analyze the skin friction reduction.

The present work deals with the calculation of the steady, two dimensional, incompressible and turbulent boundary layer over a flat plate with uniform suction and blowing, The main objective of the present work will be as follows:

- Investigation of the important parameters of the boundary layer (skin friction coefficient, displacement thickness, momentum and shape factor) in upstream and in the downstream of the slot.

- Using different positions of the slot in the range of ($X/L= 1/4, 1/2$ and $3/4$) from the leading edge with a different slot widths (0.12, 0.2 and 0.28m).

- Using different blowing and suction velocity ratios with a different pitch angles ($30^\circ \leq \alpha \leq 150^\circ$).

- Studying the profiles of time- mean velocity component at several streamwise locations for different blowing and suction velocity ratios.

PROBLEM DESCRIPTION

In the present study, a direct numerical simulation is performed to study the effect of uniform blowing or suction from a spanwise slot on a turbulent boundary layer over a flat plate see Figure (1). The free stream velocity (U_∞) was (8.6 m/s) over a flat plate of (4m) long with imposed uniform suction or blowing velocity ratios on the slot with range of ($\frac{V}{U_\infty} = \pm 0.0185, \pm 0.0463$ and ± 0.0925) for Reynolds number of (1.36×10^7) based on plate length. Also, the effects of pitch angles on the flow field are investigated in the range of ($30^\circ \leq \alpha \leq 150^\circ$).

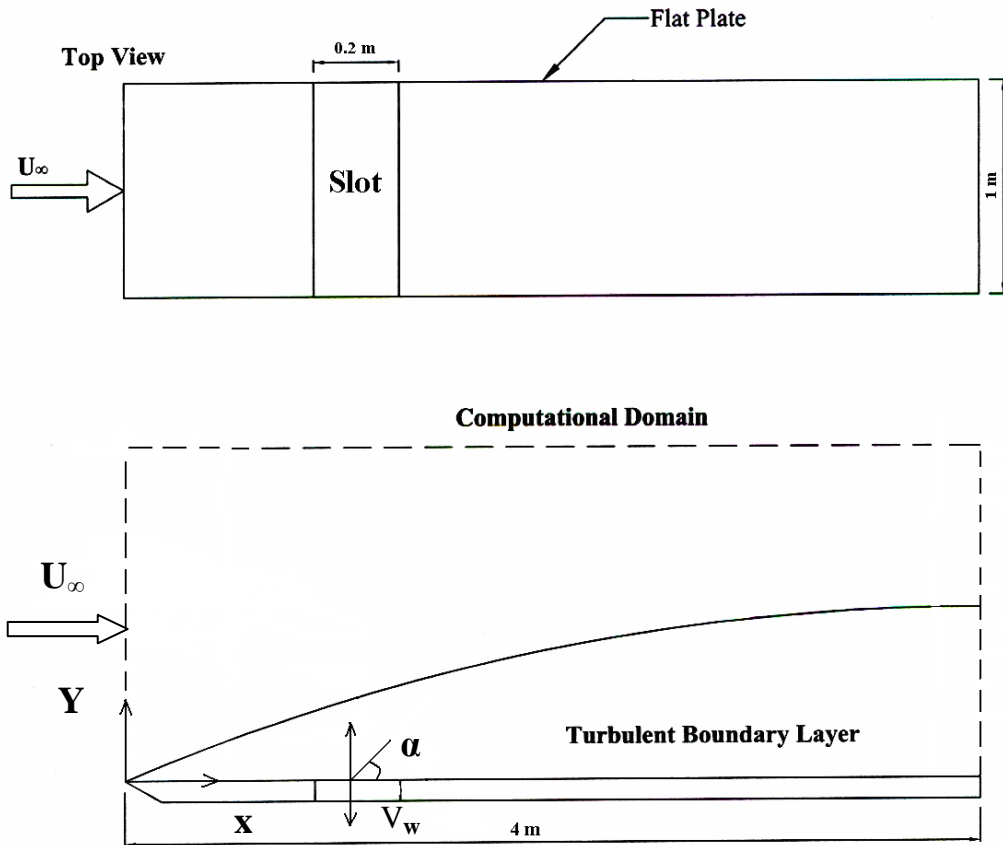


Fig. (1) Schematic diagram of computational domain

-MATHEMATICAL MODEL

The ensemble-mean equations of motion for steady state, two dimensional and incompressible flow over flat pate can be written in cartesian coordinates as follows [Awbi 1991]:

- Continuity Equation

$$\frac{\partial(\rho U)}{\partial x} + \frac{\partial(\rho V)}{\partial y} = 0 \tag{1}$$

-Momentum Equations

$$\rho U \frac{\partial U}{\partial x} + \rho V \frac{\partial U}{\partial y} = -\frac{\partial P}{\partial x} + \frac{\partial}{\partial x} \left[\mu_e \frac{\partial U}{\partial x} \right] + \frac{\partial}{\partial y} \left[\mu_e \frac{\partial U}{\partial y} \right] + \frac{\partial}{\partial x} \left[\mu_e \frac{\partial U}{\partial x} \right] + \frac{\partial}{\partial y} \left[\mu_e \frac{\partial V}{\partial x} \right] \tag{2}$$

$$\rho U \frac{\partial V}{\partial x} + \rho V \frac{\partial V}{\partial y} = -\frac{\partial P}{\partial y} + \frac{\partial}{\partial x} \left[\mu_e \frac{\partial V}{\partial x} \right] + \frac{\partial}{\partial y} \left[\mu_e \frac{\partial V}{\partial y} \right] + \frac{\partial}{\partial x} \left[\mu_e \frac{\partial U}{\partial y} \right] + \frac{\partial}{\partial y} \left[\mu_e \frac{\partial V}{\partial y} \right] \tag{3}$$

- Energy Equation

The conservation of thermal energy in the control volume [Awbi 1991]:

$$\frac{\partial}{\partial x} (\rho U T) + \frac{\partial}{\partial y} (\rho V T) = \frac{\partial}{\partial x} \left(\Gamma_e \frac{\partial T}{\partial x} \right) + \frac{\partial}{\partial y} \left(\Gamma_e \frac{\partial T}{\partial y} \right) \tag{4}$$

- Equation of a Perfect Gas

$$P = \rho RT \quad (5)$$

- Standard K-ε Model

$$\rho U \frac{\partial K}{\partial x} + \rho V \frac{\partial K}{\partial y} = \frac{\partial}{\partial x} \left[\frac{\mu_e}{\sigma_K} \frac{\partial K}{\partial x} \right] + \frac{\partial}{\partial y} \left[\frac{\mu_e}{\sigma_K} \frac{\partial K}{\partial y} \right] + \mu_t \left[2 \left(\frac{\partial U}{\partial x} \right)^2 + 2 \left(\frac{\partial V}{\partial y} \right)^2 + \left(\frac{\partial U}{\partial y} + \frac{\partial V}{\partial x} \right)^2 \right] - \rho \epsilon \quad (6)$$

$$\rho U \frac{\partial \epsilon}{\partial x} + \rho V \frac{\partial \epsilon}{\partial y} = \frac{\partial}{\partial x} \left[\frac{\mu_e}{\sigma_\epsilon} \frac{\partial \epsilon}{\partial x} \right] + \frac{\partial}{\partial y} \left[\frac{\mu_e}{\sigma_\epsilon} \frac{\partial \epsilon}{\partial y} \right] + c_{1\epsilon} \frac{\epsilon}{K} \mu_t \left[2 \left(\frac{\partial U}{\partial x} \right)^2 + 2 \left(\frac{\partial V}{\partial y} \right)^2 + \left(\frac{\partial U}{\partial y} + \frac{\partial V}{\partial x} \right)^2 \right] - c_{2\epsilon} \rho \frac{\epsilon^2}{K} \quad (7)$$

Table (1) Empirical constants in the (K-ε) [Lai and Makomaski 1989]

C_μ	$C_{1\epsilon}$	$C_{2\epsilon}$	σ_K	σ_ϵ	σ	σ_t
0.09	1.44	1.92	1.00	1.30	0.7	0.9

- BOUNDARY CONDITIONS

1. Upstream Boundary Conditions:

$$U_{up} = U_\infty \quad V_{up} = 0 \quad \epsilon_{up} = \frac{K_{up}^{1.5}}{0.005h} \quad K_{up} = 0.03(U_\infty)^2 \quad (8)$$

2. Downstream Boundary Conditions:

Normally the velocities are known only where the fluid enters the calculation domain. At downstream, the velocity distribution is decided by flow field within the domain. For incompressible flow, the gradients normal to the downstream surface of all quantities are assumed :

$$\phi_{NI,J} = \phi_{NI-1,J}$$

3. Wall Boundary Conditions:

The wall is the most common boundary encountered in confined fluid flow problems. In this section, a solid wall parallel to the u-direction is considered. The no-slip condition ($u=v=0$) is the appropriate condition for the velocity components at solid walls [Versteeg and Malalasekera 1995]. In the case of turbulent flow, the calculation of shear stress near the wall needs a special treatment. This is due to the existence of boundary layers, across which steep variation of flow properties occurs and the standard (K-ε) model becomes inadequate. In order to adequately avoid these problems, it would be necessary to employ a fine grid near the wall, which would be expensive. An alternative and widely employed approach is, to use formula which known as “wall function”

4. Free Stream Boundary Condition:

At $y = \delta$:

$$U = U_\infty, \frac{\partial u}{\partial y} = 0, P = P_\infty, T = T_\infty$$

NUMERICAL SOLUTION

For the case of steady state, incompressible and two-dimensional turbulent flow, the general equation [Patanker 1980]:

$$\frac{\partial}{\partial x}(\rho u \Phi) + \frac{\partial}{\partial y}(\rho v \Phi) = \frac{\partial}{\partial x} \left[\Gamma_{\Phi} \frac{\partial \Phi}{\partial x} \right] + \frac{\partial}{\partial y} \left[\Gamma_{\Phi} \frac{\partial \Phi}{\partial y} \right] + S_{\Phi} \quad (9)$$

Where:

$$\frac{\partial}{\partial x}(\rho U \Phi) + \frac{\partial}{\partial y}(\rho V \Phi) = \text{Convection term}$$

$$\frac{\partial}{\partial x} \left[\Gamma_{\Phi} \frac{\partial \Phi}{\partial x} \right] + \frac{\partial}{\partial y} \left[\Gamma_{\Phi} \frac{\partial \Phi}{\partial y} \right] = \text{Diffusion term}$$

S_{Φ} = Source term.

The source term (S_{ϕ}) often depends on the dependent variable (ϕ). According to [Patanker 1980] the source term can be expressed as a linear form: $S_{\phi} = S_u + S_p \phi_p$

A control finite volume method developed by [Versteeg and Malalasekera 1995] is used to discretize the governing equations. These discretization equations are solved by using SIMPLE algorithm with hybrid scheme

- the final discretised algebraic equation:

$$A_P \phi_P = A_E \phi_E + A_W \phi_W + A_N \phi_N + A_S \phi_S + S_u \quad (10)$$

Where:

$$A_p = A_E + A_W + A_N + A_S - S_p$$

Where:

$$A_E = [[0, D_e - 0.5F_e]] + [[-F_e, 0]]$$

$$A_W = [[0, D_w - 0.5F_w]] + [[F_w, 0]]$$

$$A_N = [[0, D_n - 0.5F_n]] + [[-F_n, 0]]$$

$$A_S = [[0, D_s - 0.5F_s]] + [[F_s, 0]]$$

- FURTHER NUMERICAL CALCULATION

The most important parameters for boundary layer flow, skin friction coefficient C_f , displacement thickness δ^* , momentum thickness θ , and shape factor H . these parameters are defined by the following equations [Schlichting 1968]:

$$C_f = \frac{2\tau_w}{\rho U_{\infty}^2}, \delta^* = \int_0^{\delta} \left(1 - \frac{u}{U_{\infty}}\right) dy, \theta = \int_0^{\delta} \frac{u}{U_{\infty}} \left(1 - \frac{u}{U_{\infty}}\right) dy, H = \frac{\delta^*}{\theta}, \quad (11)$$

Where: $\delta = \frac{0.376x}{\text{Re}_x^{0.2}}$

- the displacement thickness (δ^*) is computed :

$$\delta^* = \int_0^\delta \left(1 - \frac{u}{U_\infty}\right) dy = \int f(x_n) dx$$

a numerical integration methods used which is called Trapezoidel rule (or integration with unequal segments) can be used.

The general form of this method of integration is:

$$I = h_1 \frac{f(x_1) + f(x_0)}{2} + h_2 \frac{f(x_2) + f(x_1)}{2} + \dots + h_n \frac{f(x_n) + f(x_{n-1})}{2} \quad (12)$$

using the same numerical method to compute the momentum thickness.

- RESULTS AND DISCUSSIONS

Fig. (2) shows that the skin friction coefficient is changed significantly close to the region of local suction and blowing. In the case of no forcing, it is seen that, the skin friction coefficient decreases with the flow direction due to the decrease of the velocity gradient at the wall.

In the case of uniform blowing, the skin friction on the slot rapidly decreased. The near-wall streamwise vortices were lifted up by blowing, and thus interaction of the vortices with wall become weaker. Accordingly, the lifted vortices became stronger in the downstream due to less viscous diffusion (above the slot) and more tilting and stretching (downstream of the slot), resulting in the increase of the turbulence intensities as well as the skin friction downstream of the slot.

In the case of uniform suction, the skin friction on the slot increased significantly. The near-wall streamwise vortices were drawn toward the wall by suction, and thus viscous diffusion became very effective near the slot, resulting in weaker streamwise vortices in the downstream of the slot. Therefore, the turbulence intensities as well as the skin friction decreased downstream of the slot. A similar trend were observed for blowing and suction for channel flow simulations by [Park and Chio 1999] for turbulent boundary layer flow.

Fig. (3) show that the reduction of skin friction increases with increasing the velocity of blowing. Moreover, the reduction of skin friction may be related to the role of the large scale vortical structure in the vicinity of the wall. Therefore, the largest skin friction reduction is obtained at the higher blowing velocity ratio. While suction shows that, the reduction of the skin friction increases with decreasing the velocity of suction.

Fig. (4) examine the effect of the pitch angle on the reduction of skin friction. The most effective pitch angle is obtained as ($\alpha=90^\circ$), which gives the maximum reduction of skin friction reduction. While the skin friction reduction is insignificant when (α) is larger than (90°) in the case of blowing. An opposite effect is observed in the case of suction.

Fig. (5) show the variation of the skin friction coefficient at various position of the slot over a flat plate. For uniform blowing at locations 1m or 2m ($X/L=1/4$ or $1/2$) from leading edge a significantly reduction in skin friction is created, but when the blowing is moved downstream to location at 3m ($X/L=3/4$) from leading edge, a

maximum reduction in skin friction coefficient is seen. While the uniform suction shows an opposite observations.

Fig. (6) show the variation of the skin friction coefficient at different values for width of slot. For uniform blowing, the maximum reduction of skin friction is observed at width of slot (0.28 m). On the other hand, an opposite behavior is detected for suction case.

Fig. (7-11) show that, the shape factor increases with uniform blowing and decreases with uniform suction, as compared to that of the unperturbed flow. From the variation of the shape factor shown in these figures, it can be said that, uniform blowing shows the characteristics of adverse pressure gradient flow, while uniform suction shows that of favorable pressure gradient flow. The value of shape factor is different from the normal range (1.2 - 2.4) because the distribution of velocity effected by suction or blowing. Near the exit of the computational domain, the shape factors for the cases of suction are nearly the same as that of the unperturbed flow. On the other hand, the shape factors for the cases of blowing are still different from that of the unperturbed flow, meaning that the recovery distance for the shape factor due to blowing is longer than that due to suction. For uniform blowing the shape factor increases with increasing the velocity ratios, pitch angle, width of slot and when the slot moves downstream. An opposite observations are obtained for the case of suction. This is consistent with observation of numerical results of Park and Chio [1999].

Fig. (12-23) show the limiting behavior of turbulence intensities (uu and vv) and the Reynolds shear stress (uv) at the blowing and suction walls. Its clear that, uniform suction decreases the magnitudes of the velocity fluctuations, while uniform blowing increases them near the slot. It is also seen that near the slot for suction the profile of the turbulence intensities shifts toward the wall, and for blowing away from the wall, but at downstream of the slot, the an opposite behavior is observed. This is consistent with the results of Chung and Sung [2001]. The increases or decreases in the maximum values of turbulence intensities and Reynolds shear stress depend on the blowing or suction velocity ratios. Above the slot, in case of blowing, when increased the velocities of blowing, the (uu) and (uv) are more decreased than (vv), while (vv) is more decreased than (uu) and (uv) in the case of suction. The same behavior opposerved at different pitch angles, different slot widths and different positions of the slot for uniform blowing and suction.

Near the wall behavior of the streamwise velocity profiles in term of $\left(U^+ = \frac{U}{u_\tau} \right)$ are shown in Fig. (24). Here, the local friction velocity $\left(u_\tau = \sqrt{\frac{\tau_w}{\rho}} \right)$ is calculated along the streamwise direction over a flat plate. For the case of blowing, the velocity retardation at the wall leads to a reduction in the local skin friction coefficient (C_f) because of the small friction velocity and this reduction is increased with increasing velocity of blowing. The opposite is observed for the case of the suction.

Fig. (25) show the streamwise mean velocity profiles for forcing angle in the range ($30^\circ \leq \alpha \leq 150^\circ$). For uniform blowing, the forcing angle of ($\alpha \leq 90^\circ$) caused more significant reduction on (U^+), while an opposite behavior is observed in the case of the suction.

Fig. (26) for uniform blowing, the slot location at 3m ($X/L=3/4$) from leading edge gives better results for mean velocity than the locations 1m or 2m ($X/L=1/4$ or $1/2$) from leading edge, but in the same location the flow does not appear significantly affected by the suction .

Fig. (27) show the predicted mean velocity profile in wall coordinates at different values of slot widths. Wider width of slot appears to be the most effective choice to reduce mean velocity profile; a reverse effect is showed for the case of the suction.

COMPARISON OF THE RESULTS

The numerical result of the present work is compared with available numerical result and experimental data. Some of the results show a discrepancy. This difference seems to be due to different magnitudes of blowing and suction velocities applied and also due to different widths of blowing and suction areas.

In Fig. (28), the predicted skin friction coefficient is compared with the numerical data of [Park and Chio 1999]. As displayed in figures, the present simulation shows good agreement with the numerical data for two cases blowing and suction.

Fig. (29) show the comparison of the shape factor with the numerical results of [Park and Chio 1999]. Satisfactory predictions have been obtained with the present results and a good agreement with available numerical data is observed

It can be seen from the Fig. (30), that the present prediction of skin friction coefficient is in a reasonable agreement with the carefully reviewed numerical data of [Munem 2004].

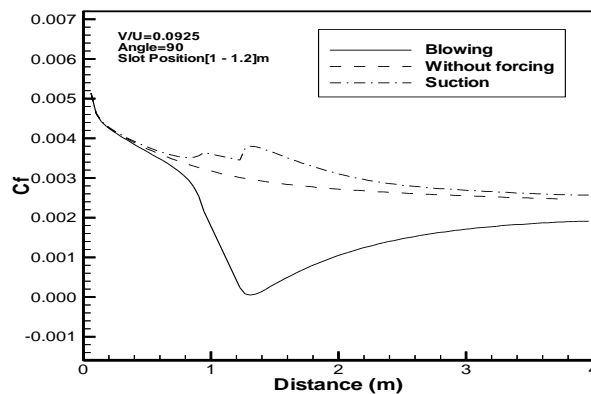


Fig. (2) Streamwise variation of skin friction coefficient for blowing, suction and without forcing.

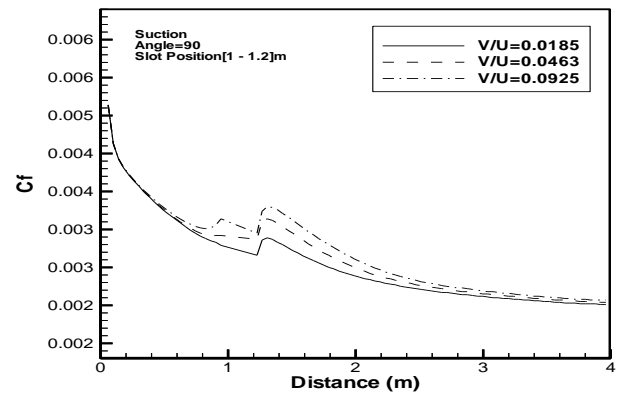
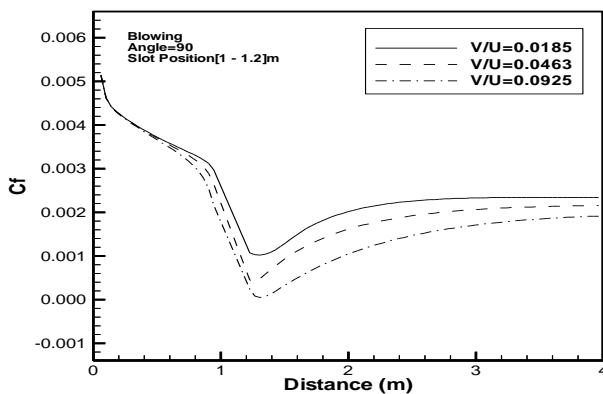


Fig. (3) Variation of skin friction coefficient for various velocity ratios

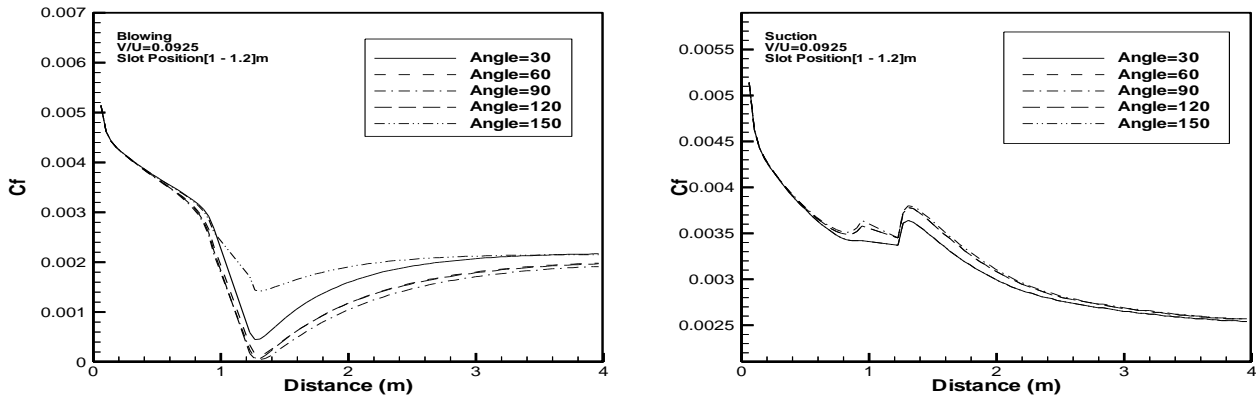


Fig. (4) Variation of skin friction coefficient at various pitch angles.

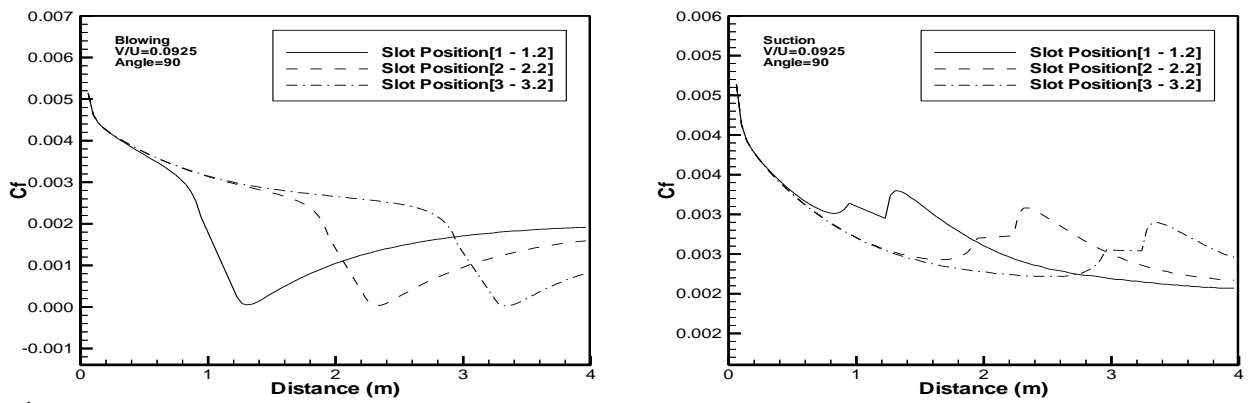


Fig.(5) Variation of skin friction coefficient at various positions of the slot.

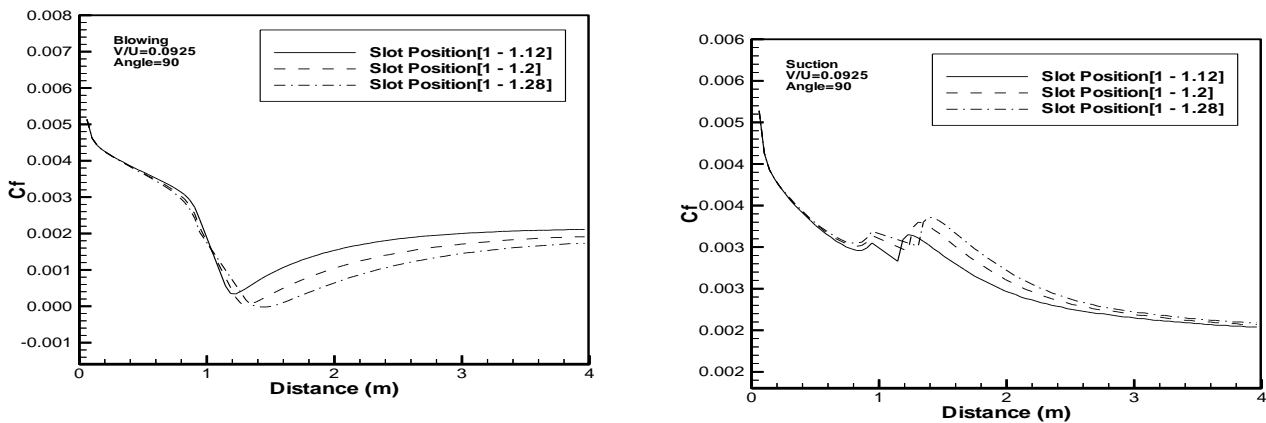


Fig. (6) Variation of skin friction coefficient at different values for width of slot.

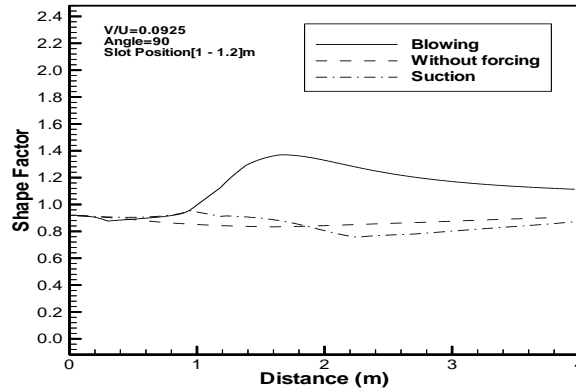


Fig. (7) Streamwise variation of shape factor for blowing, suction and without forcing.

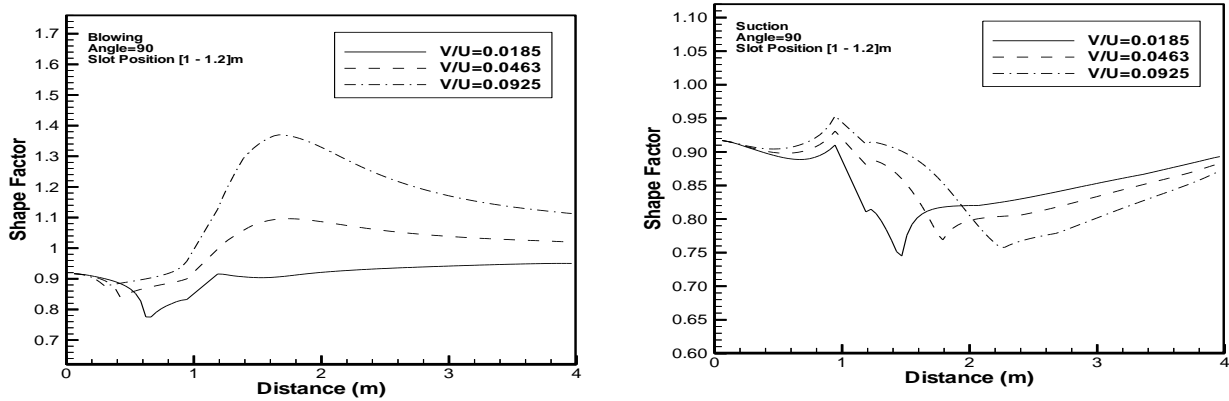


Fig. (8) Variation of shape factor for various velocity ratios.

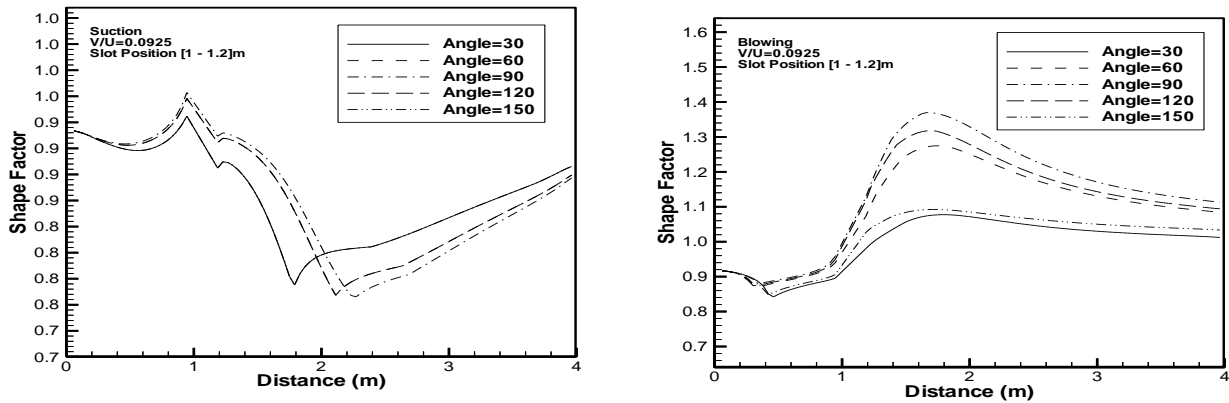


Fig. (9) Variation of shape factor at various pitch angles.

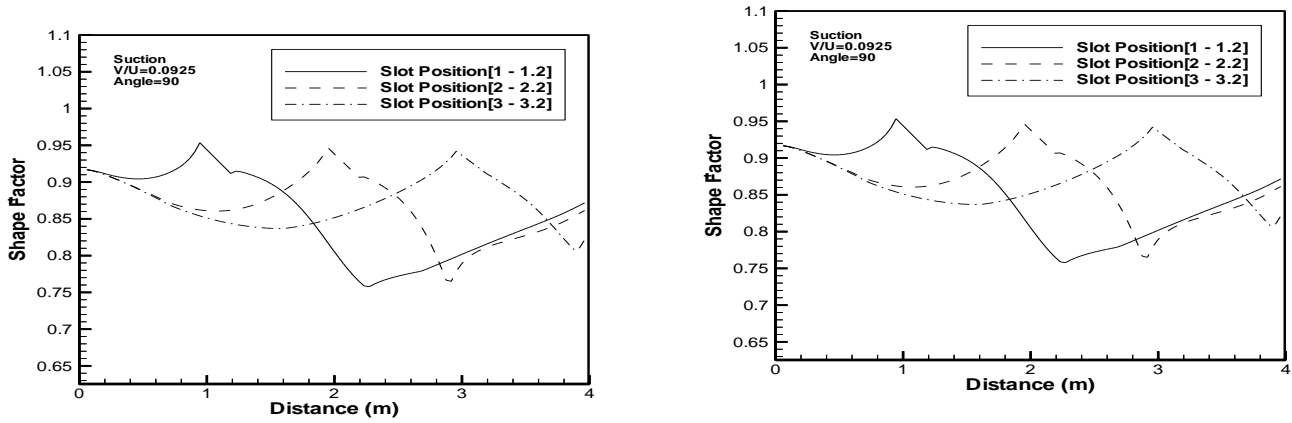


Fig. (10) Variation of shape factor at various positions of the slot.

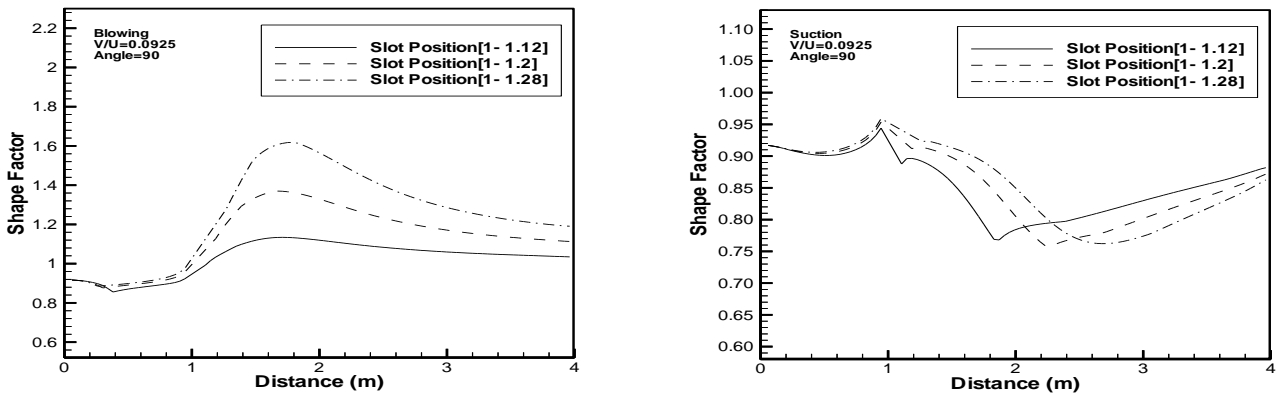


Fig. (11) Variation of shape factor at different values for width of slot.

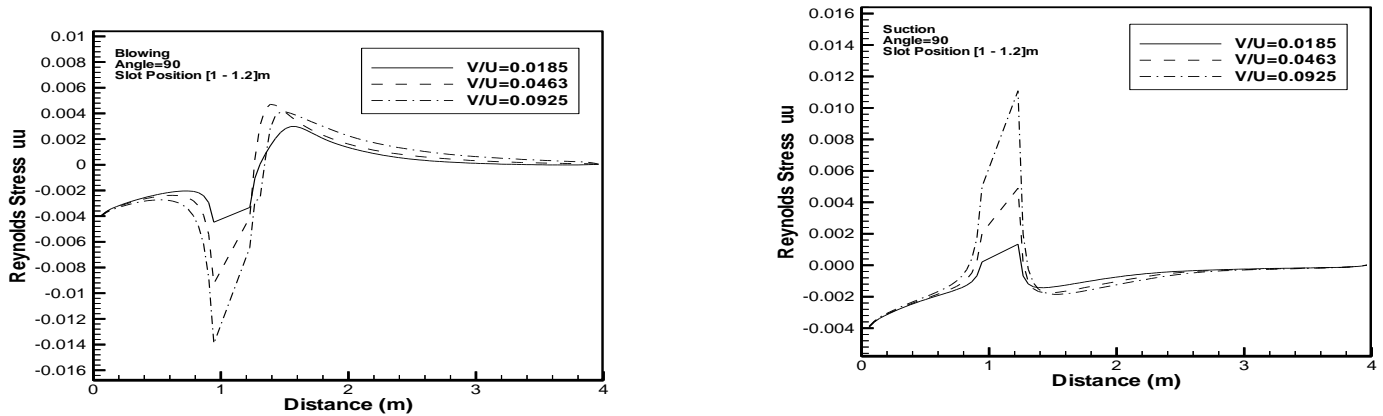


Fig. (12) Variation of the Reynolds stress (uu) for various velocity ratios.

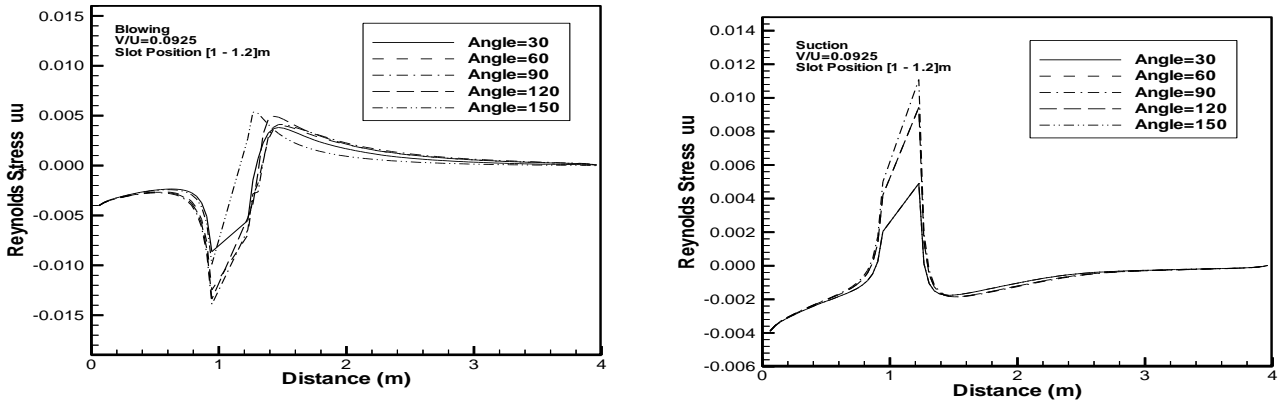


Fig. (13) Variation of the Reynolds stress (uu) at various pitch angles.

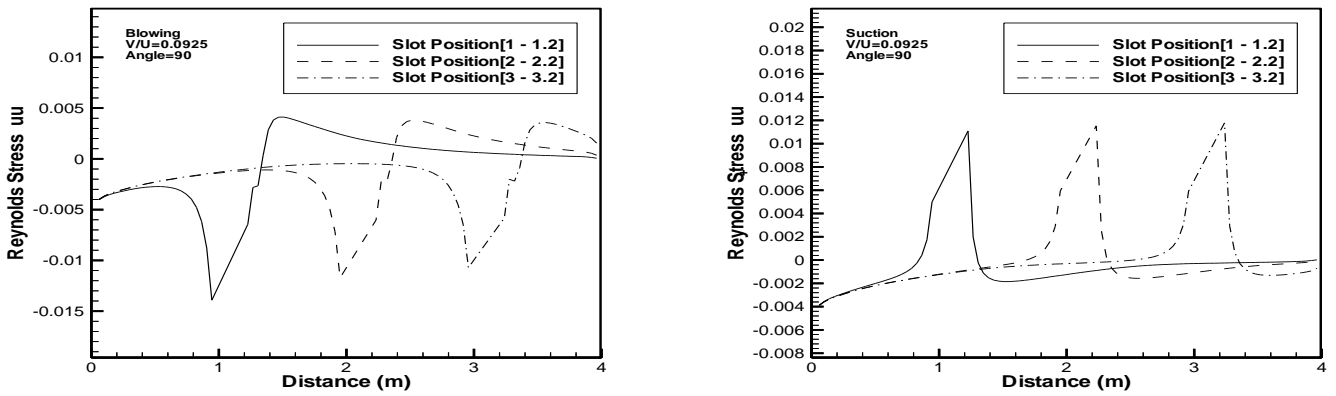


Fig. (14) Variation of the Reynolds stress (uu) at various positions of slots.

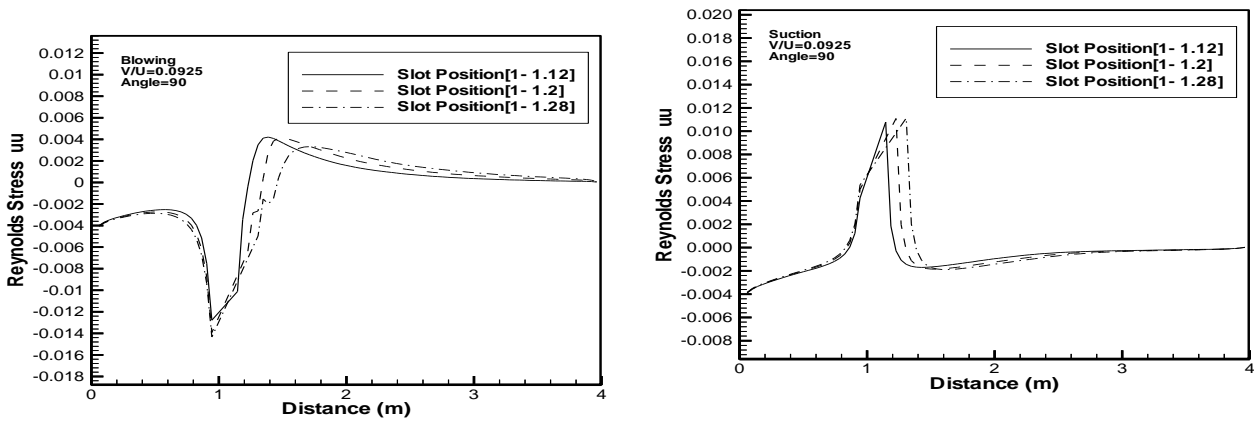


Fig. (15) Variation of the Reynolds stress (uu) at different values for width of slot.

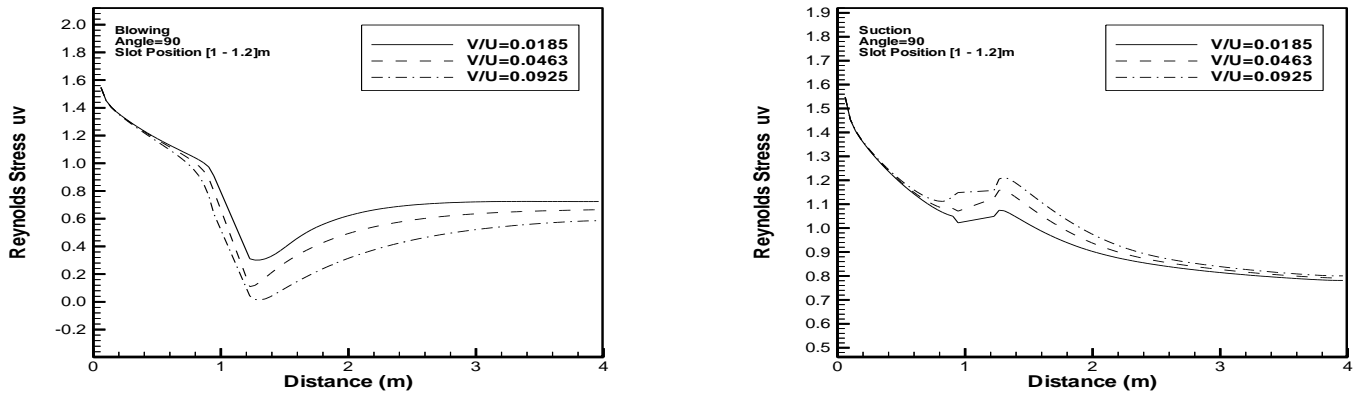


Fig. (16) Variation of the Reynolds stress (uv) for various velocity ratios.

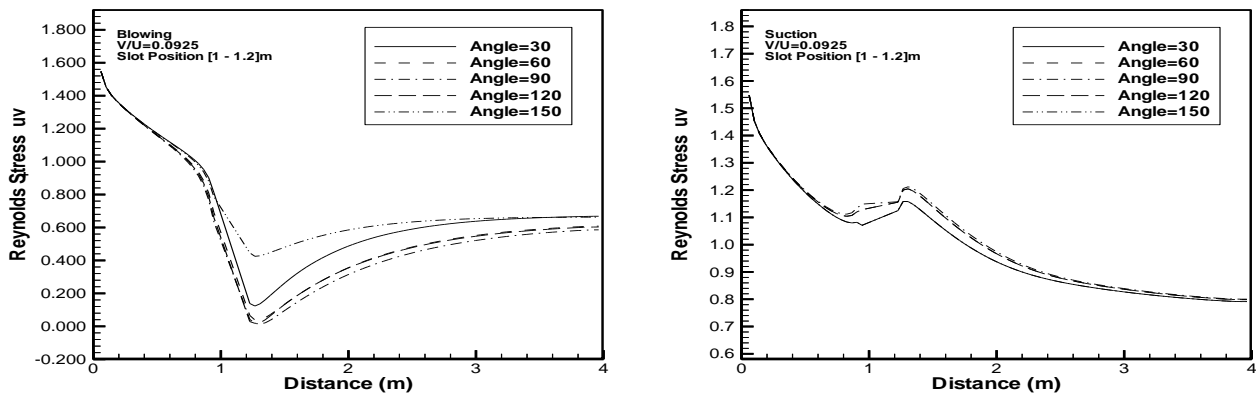


Fig. (17) Variation of the Reynolds stress (uv) at various pitch angles.

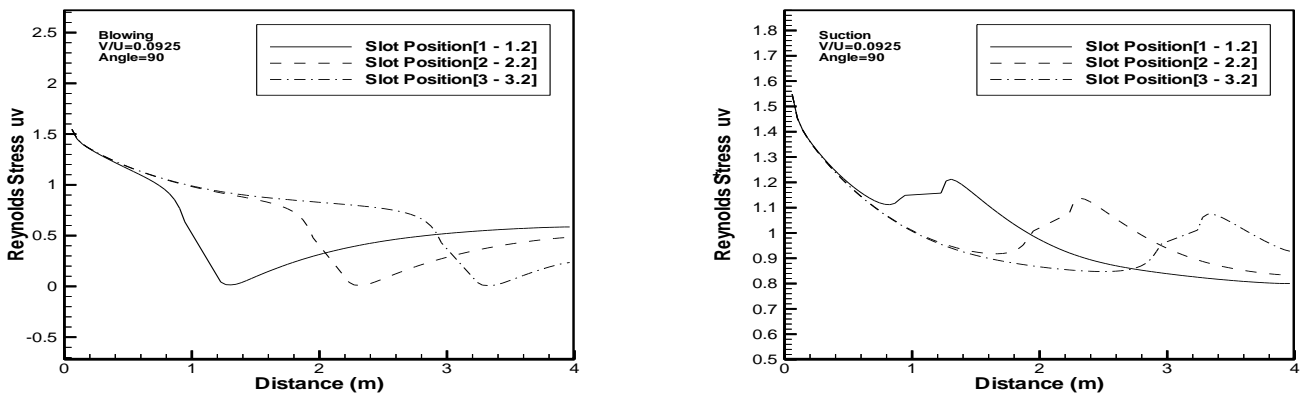


Fig. (18) Variation of the Reynolds stress (uv) at various positions of the slot.

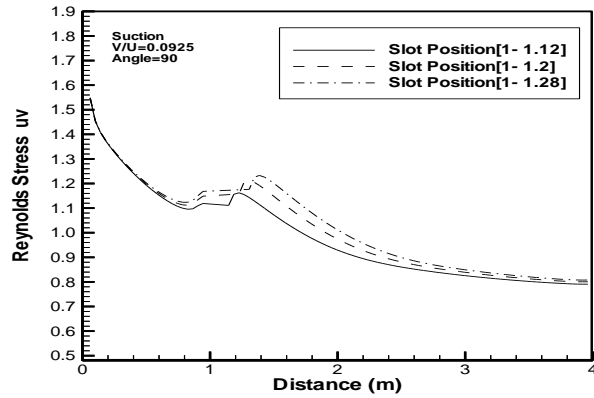
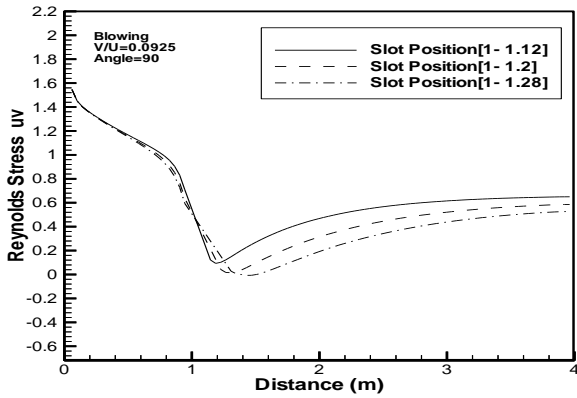


Fig. (19) Variation of the Reynolds stress (uv) at different values for width of slots.

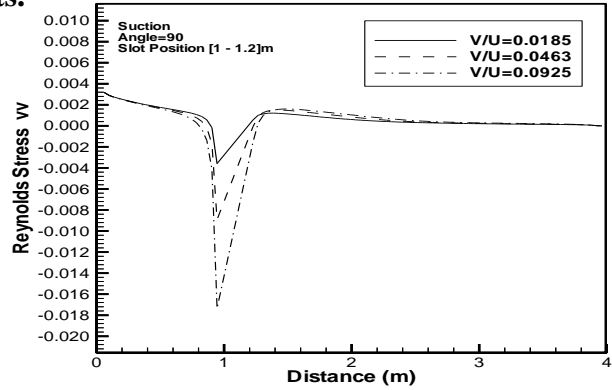
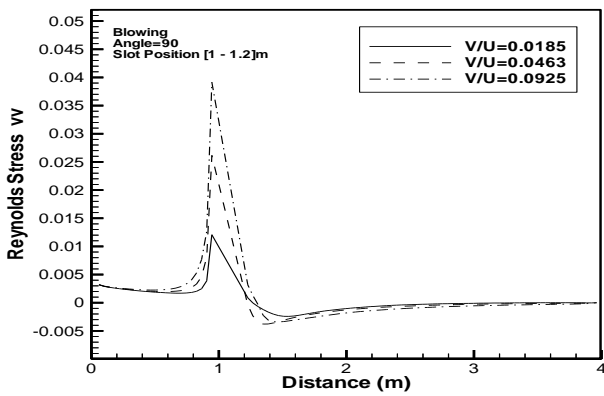


Fig. (20) Variation of the Reynolds stress (vw) at various velocity ratio.

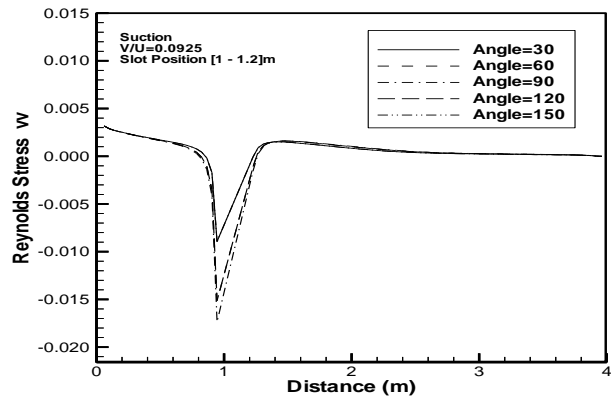
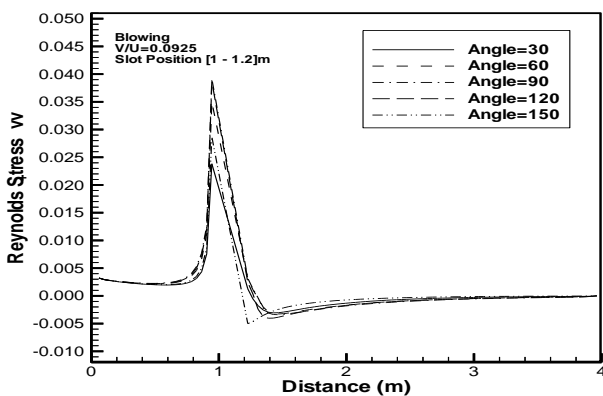


Fig. (21) Variation of the Reynolds stress (vw) for pitch angles.

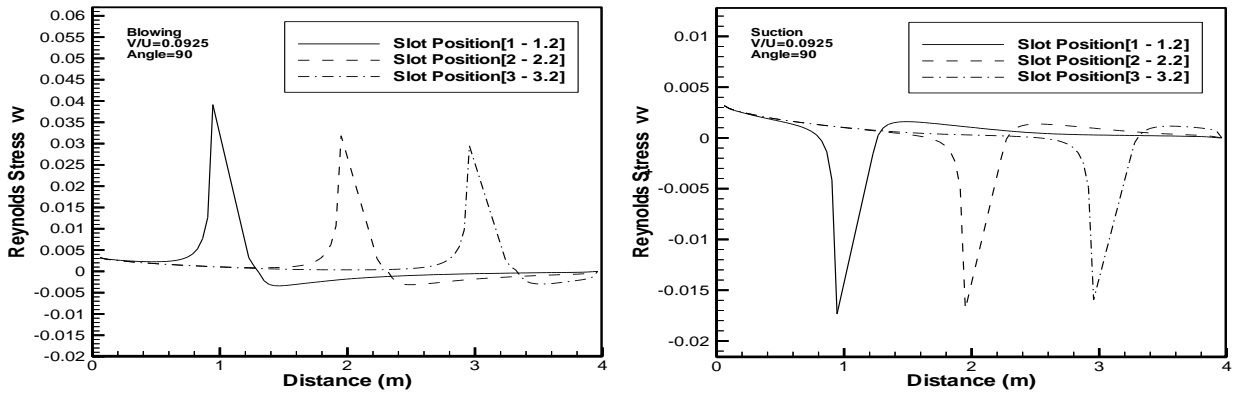


Fig. (22) Variation of the Reynolds stress (vw) at various positions of the slot .

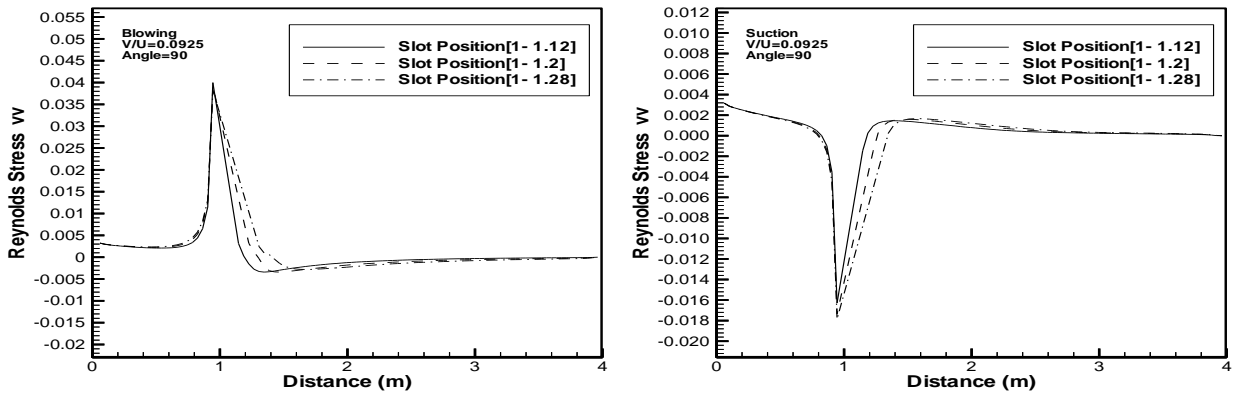


Fig. (23) Variation of the Reynolds stress (vw) at different values for width of slot.

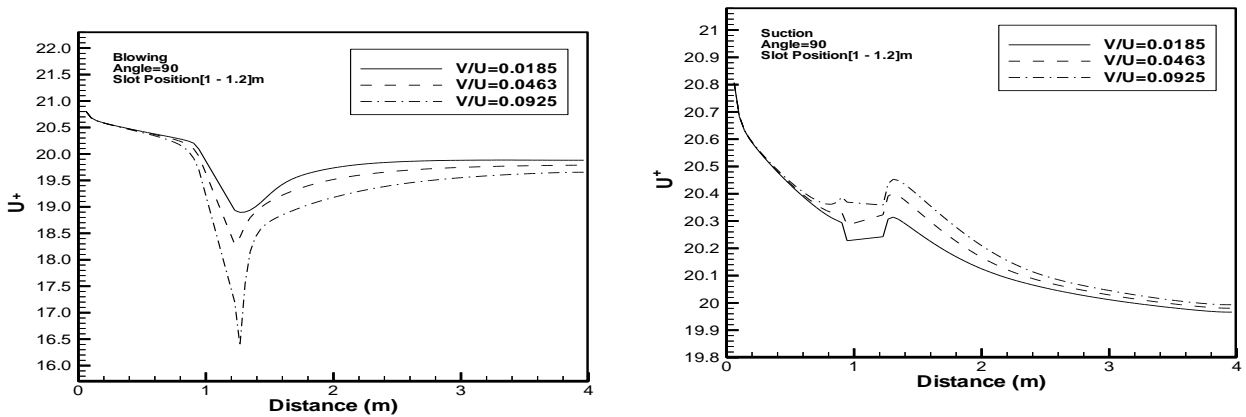


Fig. (24) Variation of mean velocity profiles in wall coordinates at various velocity ratios.

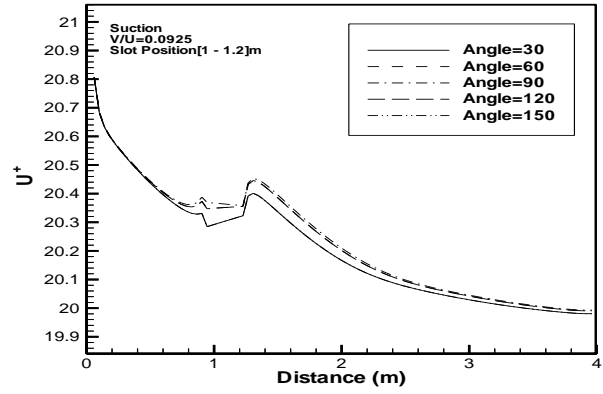
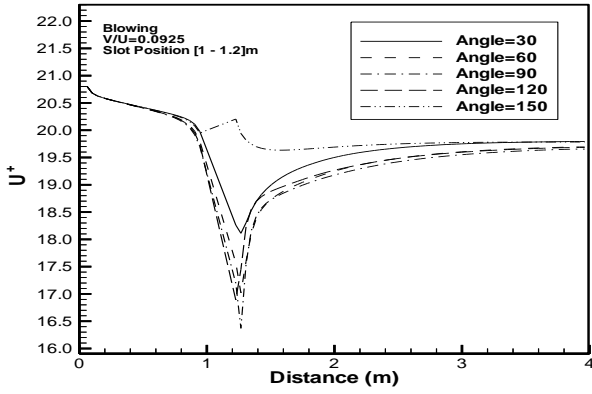


Fig. (25) Variation of mean velocity profiles in wall coordinates at various pitch angles.

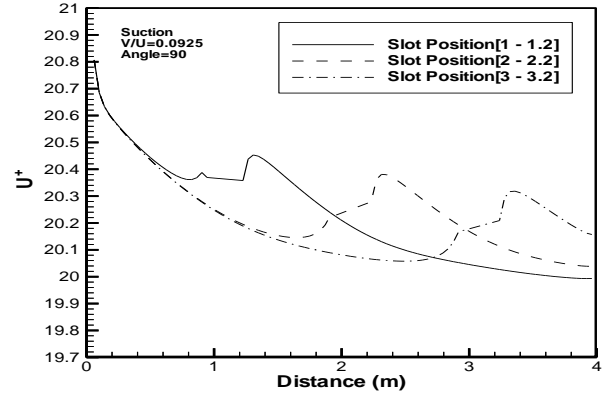
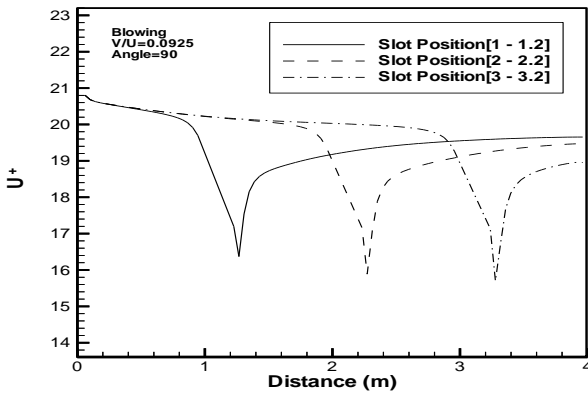


Fig.(26)Variation of mean velocity profiles in wall coordinates at various positions of the slot .

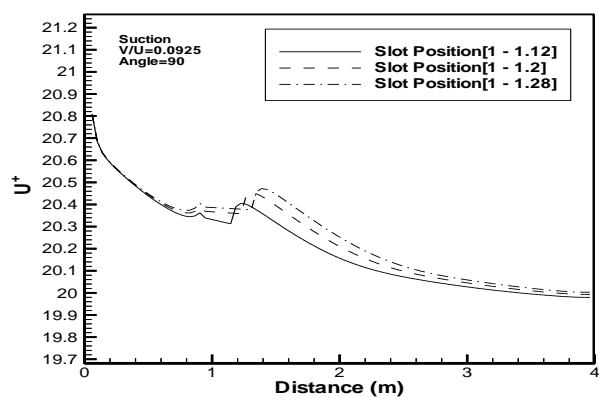
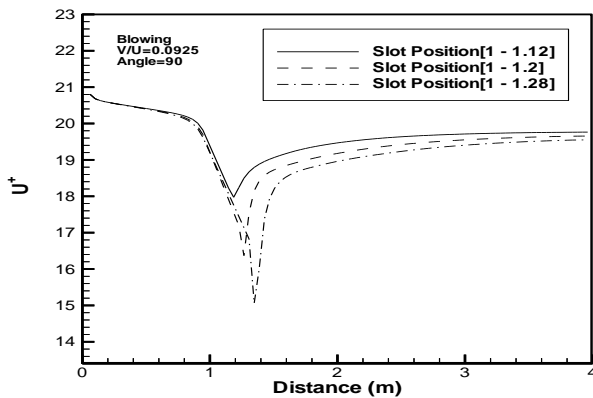


Fig. (27) Variation of mean velocity profiles in wall coordinates at different values for width of slot .

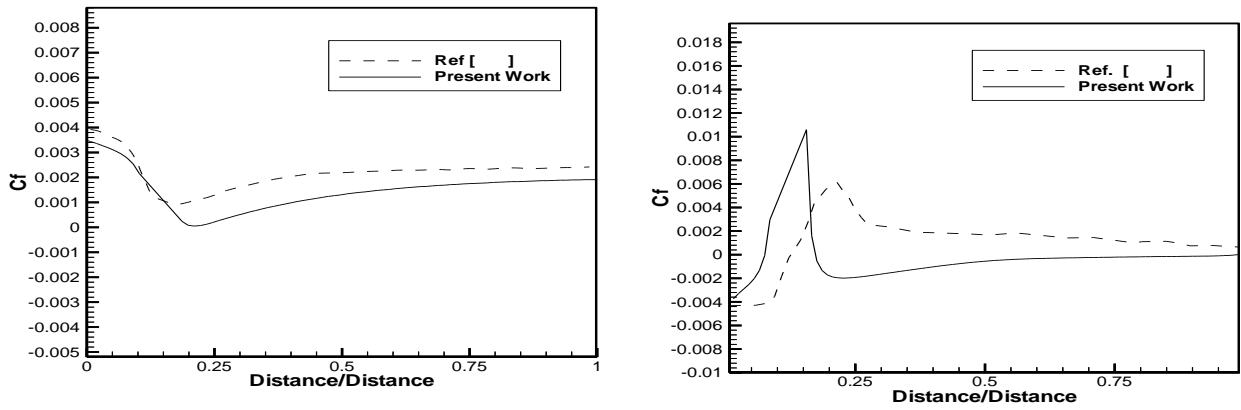


Fig. (28) Comparison of skin friction coefficient with numerical results of [Park and Chio 1999].

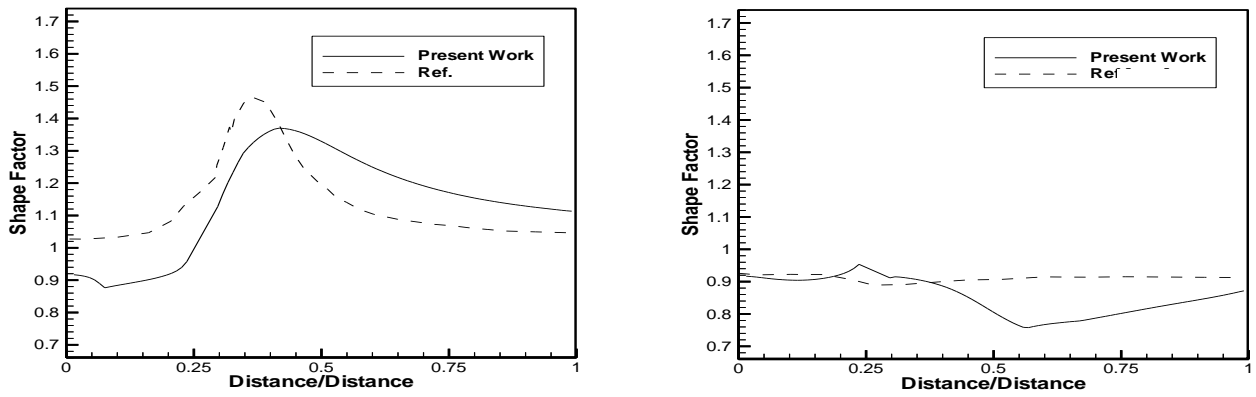
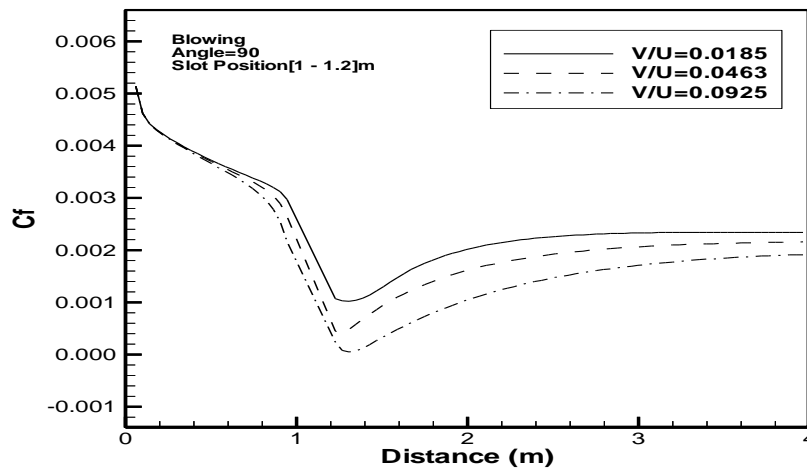
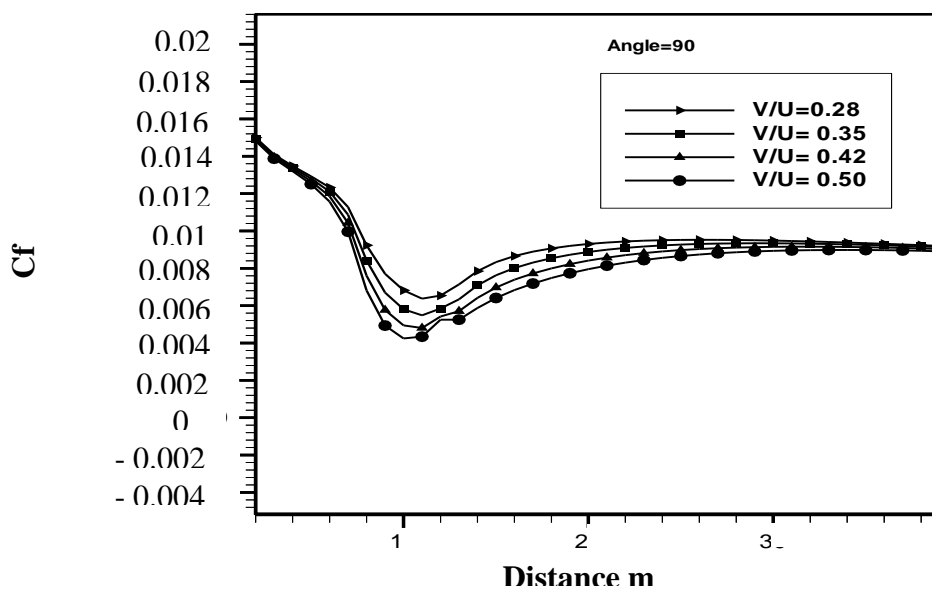


Fig. (29) Comparison of the shape factor with numerical results of [Park and Chio 1999].



Present work



Reference [Munem 2004].

Fig. (30) Comparison of skin friction coefficient with numerical results of [Munem 2004]

CONCLUSION

- In the case of blowing, near the slot, the skin friction coefficient decreases and increases in the downstream of the slot. While a reverse action is observed for the case of suction.
- The largest skin friction reduction is obtained at the higher blowing velocity ratios for uniform blowing.



- The most effective pitch angle is obtained as ($\alpha=90^\circ$) which gives a maximum reduction in skin friction coefficient.
- For uniform blowing, location of slot at 3m ($X/L=3/4$) from leading edge is more effective location for reduction of skin friction coefficient, while a reverse action is observed for the case of uniform suction.
- It was found that, a width of slot equal (0.28m) gives the maximum reduction in skin friction coefficient for uniform blowing.
- Blowing causes a decrease in boundary layer thickness and increase in shape factor, while suction causes a reverse effect. The increase or decrease is proportional to the velocity ratios, positions of slot, and widths of slot.
- Above the slot, in case of blowing, when increased the velocities of blowing, the (uu) and (uv) are more decreased than (vv), while (vv) is more decreased than (uu) and (uv) in the case of suction.
- For uniform blowing, $[U^+]$ decrease with increasing velocity ratios, pitch angles, positions of slot and widths of slot. While a reverse action is observed for the case of the suction.

REFERENCES

- Awbi, H. H., "Ventilation of Building", Department of Construction Management and Engineering, University of Reading, London (1991).
- Kim, K. and Sung, J. H., "Effect of Periodic Blowing from Span Wise Slot On A Turbulent Boundary Layer", AIAA. Journal, Vol.41, No.10, PP.196-1924, October (2003).
- Krogsted, P. A. and Kourakine, A., "Some Effects of Localized Injection on the Turbulence Structure in a Boundary Layer", Physics of Fluid, Vol. 12, No. 11, pp.2990-2999, November (2000).
- Lai, K. Y. M., and Makomaski, A. H., "Three Dimensional Flow Pattern Upstream of a Surface Mounted Rectangular Obstruction", Transactions of the ASME, Journal of Fluids Engineering, Vol. 111, pp. 449-456, December (1989).
- Munem, D. S., "Effect of suction and Blowing on the Flow Over A Flat Plate ", MSC. Thesis, Mechanical Engineering Department, University of Baghdad, October (2004).
- Park, j. and Choi, H., "Effects of Uniform Blowing or Suction from a Span Wise Slot on a Turbulent Boundary Layer Flow", Journal Physics of Fluids, Vol.11, No.10, pp. 3095-3105, October (1999).
- Park, Y.S., Park, S.H., and Sung, H. J., " Measurement of Local Forcing on a Turbulent Boundary Layer using PIV", Journal Experiments in Fluids, Vol.34, PP. 697-707, April (2003).

- Patankar, S. V., "Numerical Heat Transfer and Fluid Flow", Hemisphere Publishing Corporation, Taylor & Francis Group, (1980).
- Schlichting, H., "Boundary Layer Theory", Sixth Edition, McGraw- Hill Book Company, New York (1968).
- Versteeg, H.K., and Malalasekera, W., "An Introduction to Computational Fluid Dynamics-The finite volume method", Longman group Ltd., (1995).